NanoAnalysis
An International Journal
Available online at: www.jnanoanalysis.net or www.jnanoanalysis.com

IR and UV Spectroscopic Analysis of C_{20} Carbon Nanostructures

Mehdi Zamani[1,3]*, Ahmad Motahari[2], Hossein A. Dabbagh[3], Hossein Farrokhpour[3]

1) Department of Chemistry, Malek-ashtar University of Technology, Shahin-shahr P.O. Box 83145/115, Islamic Republic of Iran
2) Faculty of Chemistry, University of Mazandaran, P.O. Box 453, Babolsar, Islamic Republic of Iran
3) Department of Chemistry, Isfahan University of Technology, Isfahan 84156-83111, Islamic Republic of Iran

Abstract

Infrared (IR) and ultraviolet (UV) spectroscopic analysis of eight structural isomers of C_{20} carbon nanostructures, i.e. ring, tadpole, bow-tie, dumb-bell, spiro, propellane, bowl and cage, were performed at different levels of theory including semi-empirical (AM1 and PM3), Hartree-Fock (HF/6-31++G, 6-31++G**) and density functional theory (B3LYP/6-31++G, 6-31++G**). A broad range of IR spectra (400-2700 cm^{-1}) is covered by C-C bending vibrations (low frequency region) and C-C stretching vibrations (high frequency region) in almost all isomers. The absorption maximum (λ_{max}) in UV spectra for bowl and cage isomers appears below 300 nm and for cyclic isomers above it. These results show that IR and UV spectra are useful tools for identification of C_{20} structural isomers.

Keywords: C_{20} Isomers; Fullerenes; Infrared; UV spectra

1. Introduction

Carbon clusters are fascinating examples of the richness and variety of carbon chemistry. Recently, Prinzbach et al. provided experimental evidence for the existence of three different C_{20} isomers (cage, bowl and ring) in the gas phase (1,2). Also, Wang et al. reported the synthesis of the crystallized solid form of cage (fullerene) isomer by the Ar^+ beam irradiation of polyethylene sample (3).

Even though, the experiments are unequivocally consistent with the existence of those structures, there is no clear evidence as to which one is the most stable isomer. Calculation of the relative energies of the different C_{20} isomers is a great theoretical challenge. For example, AM1 (4), SCF (self-consistent field) approximation (5,6), GC-LDA (gradient-corrected local density approximation) (7), HF (8,9), BLYP (Becke-Lee-Yang-Parr) generalized gradient approximation (8,10), B3LYP (11,12) and HCTH (10) methods predict ring structure as optimal for C_{20}, whereas MP2 (MØller-Plesset second-order perturbation) (4), uncorrected LDA (8,10), LSD (local spin density) approximation (13) and BP (Becke-Perdew) (13) methods predict the cage structure as having the lowest energy. Finally, high-level MP2 calculations

* Corresponding author. *E-mail address:* m.zamani@ch.iut.ac.ir.

(14,15), QM (quantum mechanic) (16), DMC (diffusion Monte Carlo) (9) and CCSD (coupled-cluster singles and doubles) (6) calculations predict the bowl is the most stable isomer. Furthermore, there are some reports in the literature dealing with the electronic (17-24), thermodynamic (25), vibrational (14,21,22,26-28), nuclear magnetic resonance (NMR) (10) and aromatic (12) properties as well as energetic studies for C_{20} isomers. These results mostly restricted to famous C_{20} isomers such as ring, bowl and cage with low accuracy level of vibrational analysis using LDA, BLYP, AM1, MNDO and PM3 methods (14,22,26-28). Also a number of new quantum chemical calculations have been extended to a more number of C_{20} isomers including cyclic, planar (11,12) and cage (29) in recent years. Also a new inter conversion mechanism for these isomers have been reported (30-32).

In this study we report the IR spectra for eight C_{20} isomers (monocyclic, bicyclic and tricyclic rings, bowl and cage) at different levels of calculations including B3LYP (6-31++G, 6-31++G**) and HF (6-31++G, 6-31++G**) and compared them with the results obtained using semi-empirical methods (AM1, PM3). Also, the UV spectral data is reported for C_{20} isomers for the first time. Finally, we show that these data are useful tools for geometry identification of the different C_{20} nanostructures.

2. Computational details

The eight isomers of C_{20} were optimized without any symmetry constraint using the different theoretical methods including B3LYP (6-31++G, 6-31++G**) and HF (6-31++G, 6-31++G**) as well as semi-empirical procedures (AM1 and PM3). The Keyword opt=tight was included to increase the convergence criteria in order to obtain reliable geometries for isomers. The IR spectra were calculated using these levels of theory. Also, the UV spectral data were predicted via RCIS (Restricted Configuration Interaction Singlet) method at 6-31G basis set for both optimized geometries of the HF and B3LYP calculations. All calculations were carried out using Gaussian-03 software package (33).

3. Results and discussion

Infrared spectra and vibrational modes of C_{20} isomers including monocyclic rings (ring and tadpole), bicyclic rings (bow-tie, dumb-bell and spiro), tricyclic ring (propellane), bowl and cage calculated at the B3LYP level of theory are presented in Figures 1-10. As shown, the tadpole isomer is composed of ring and tail carbon atoms and the bow-tie, dumb-bell and spiro isomers consist of two monocyclic rings connecting by a four-member ring, cumulenic double bonds and a tetrahedral carbon atom, respectively. In propellane isomer three rings are connected by two carbon atoms.

A broad range of IR spectrum, 400 to 2700 cm^{-1}, is covered by C-C bending vibrations (low frequency region) and C-C stretching vibrations (high frequency region) for all the isomers. The IR spectra, calculated at different levels of theory, are not the same and occasionally there is a big shift in the peaks. Figure 1 shows IR spectra of C_{20} isomers calculated at B3LYP/6-31++G level of theory. Active vibrational modes (with the intensity higher than 10) are shown in Figures 3-10. In the following, the vibrational frequencies calculated by this method are compared with the corresponding bands calculated by other methods i.e. B3LYP/6-31++G**, HF/6-31++G, HF/6-31++G**, AM1 and PM3. Also, we introduce some IR bands as a characteristic of each C_{20} isomer; in other words, we determine some specific functional groups consist of carbon atoms for each isomer and then interpret the IR spectra according to them (Figure 2).

IR spectrum of ring isomer is very simple (Figure 3). Two scissoring vibrational modes are responsible for the appearance of base peak at 188 cm^{-1} by B3LYP/6-31++G method. In one of these modes C6-C9 and C10-C16 atoms are active while, in the other mode C1-C4 and C11-C14 are active (Figure 3a). This band is observed at 714, 603, and 691 cm^{-1} in HF/6-31++G, AM1, and PM3 calculations, respectively. The short band appeared at 551 cm^{-1} (B3LYP/6-31++G) is assigned to the ring breathing vibration (Figure 3b). This vibrational mode is seen at 566 and 614 cm^{-1} for HF/6-31++G and PM3, respectively but, is not active at AM1 method. The third band is assigned to in plane symmetric stretching vibration of ring carbon atoms and is observed above 2000 cm^{-1} by four levels of theory considered (Figure 3c). As seen in Figure 3, there are two vibrational modes for each band in IR spectrum because some carbon atoms are active and inactive.

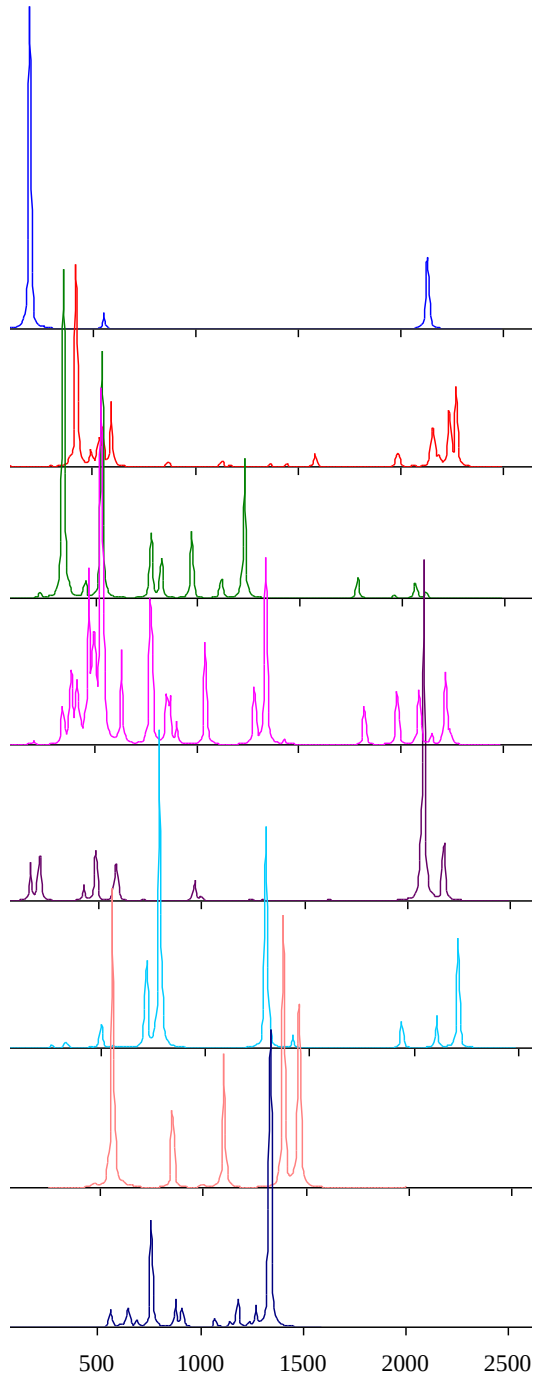

Fig. 1. IR spectra of C_{20} isomers i.e. ring, tadpole, bow-tie, dumb-bell, spiro, propellane, bowl and cage (from top to bottom) calculated via B3LYP/6-31++G method

Tadpole isomer has two specific functional groups (Figure 2): carbonic tail C1=C2 and ∠C3-C2-C20 angle which are a characteristic of this structure. None of these two characters are base peaks in the calculated IR spectrum at HF and B3LYP levels. The base peak at HF/6-31++G calculation is observed at 581 cm^{-1} which is due to simultaneous bending vibration of ring and tail carbon atoms (Figure 4a). The bands corresponding to tadpole functional groups include two bending vibrations of ∠C3-C2-C20 (494, 547 cm^{-1}), (Figures 4c, e) and a stretching vibration of C1=C2 (1584 cm^{-1}), (Figure 4g), was calculated by

B3LYP/6-31++G method. These modes at HF/6-31++G level are observed at 690, 774, and 1790 cm^{-1}, respectively. The base peak at AM1 and PM3 level is assigned to the stretching vibrations of C1=C2 which is seen at 1852 and 1900 cm^{-1}, respectively. In the plane symmetric bending vibration of ∠C3-C2-C20, calculated at AM1 and PM3 levels, are appeared at 718 and 717 cm^{-1}, respectively. The first stretching vibrations of tadpole carbon atoms at B3LYP/6-31++G level are observed at 1985 cm^{-1} (Figure 4h). Also, a new band is seen at 1634 cm^{-1} by AM1 method, assigned to the simultaneous symmetric stretching vibration of ring and tail atoms of tadpole molecule. These results show that removing one carbon atom from C_{20} ring isomer (which leads to forming tadpole isomer) causes the stretching frequencies of ring to be shifted down 2000 cm^{-1}. The last stretching vibration mode for tadpole's ring is observed at 2271 cm^{-1} at B3LYP/6-31++G level (Figure 4l). This mode is seen as two symmetric and asymmetric stretching vibrations in HF/6-31++G and PM3 calculations. The band corresponding to symmetric stretching vibration is observed at higher frequencies.

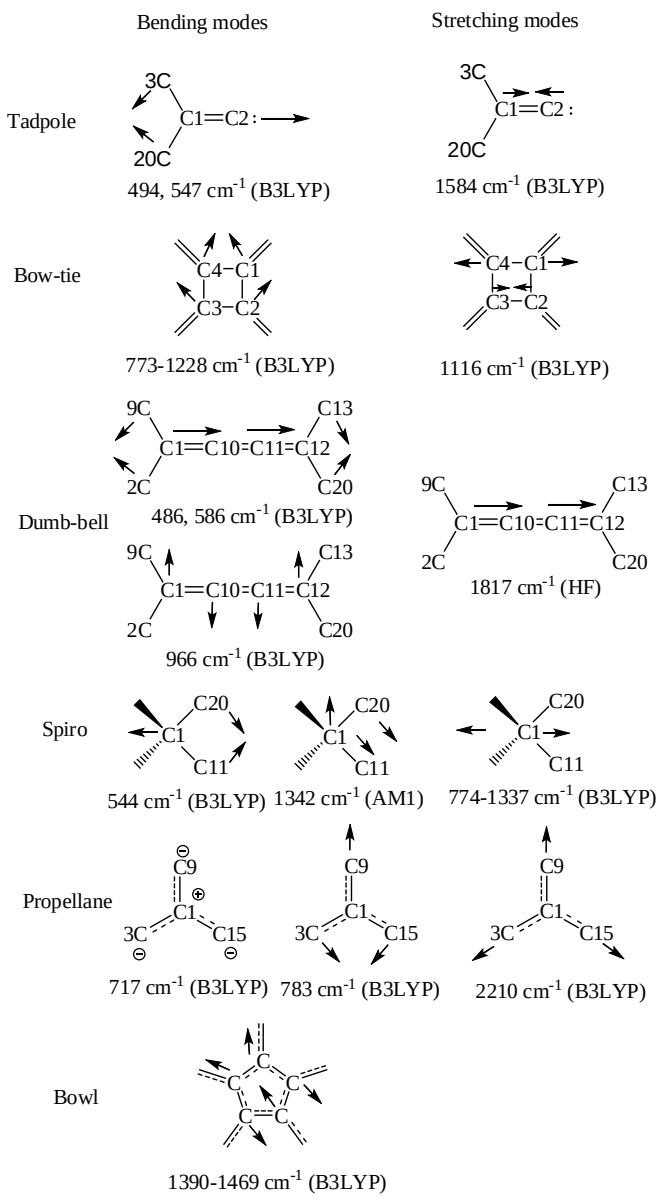

Fig. 2. Functional groups of C_{20} isomers and their vibrational frequencies

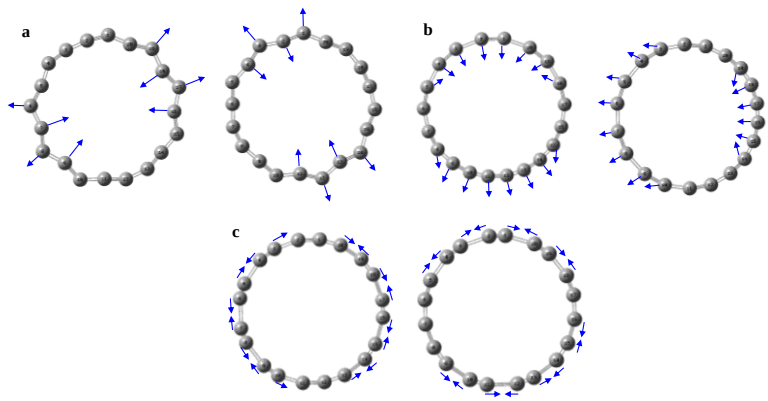

Fig. 3. Vibrational modes for ring isomer at B3LYP/6-31++G level of theory

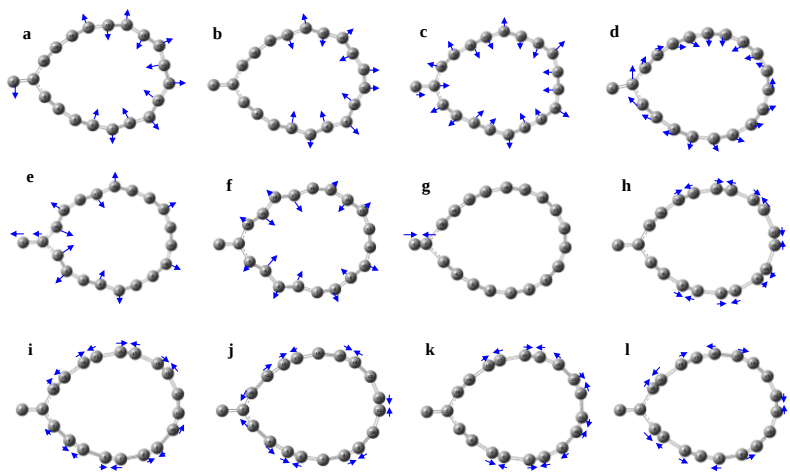

Fig. 4. Vibrational modes for tadpole isomer at B3LYP/6-31++G level of theory

Bow-tie isomer has a functional group consists of a four-member ring (Figure 2) which is responsible for all observed peaks in the range of 773-1228 cm^{-1} at B3LYP/6-31++G level (Figures 5d-h). These bands can be used as finger print for this isomer. The simultaneous bending vibration of four-member ring along with the rings around it results in 773, 823, 970, and 1228 cm^{-1} bands at B3LYP/6-31++G level (Figures 5d, e, f, h). The observed band at 1116 cm^{-1} (Figure 5g) is assigned to the asymmetric stretching vibration of four-member ring carbon atom. The base peak in all calculation methods is related to the scissoring vibration of carbon atoms belonging to the bigger rings. This vibrational band is seen at 342 cm^{-1} at B3LYP/6-31++G level (Figure 5a) and at 623, 592, and 645 cm^{-1} by HF/6-31++G, AM1, and PM3 methods, respectively (Figure 5c). Comparison this mode with corresponding mode related to the scissoring vibration of ring isomer shows a shift to higher frequencies (188 to 342 cm^{-1}) at B3LYP/6-31++G level and also is seen other methods too. The observed band at 1783 cm^{-1} at B3LYP/6-31++G level is assigned to a combination of bending vibration of four-member ring and the stretching vibration of bigger rings (Figure 5i). The pure symmetric stretching vibration of carbon atoms belongs to bigger ring, appear at 2066 cm^{-1} by B3LYP/6-31++G method (Figure 5j). This band is seen at 2299 cm^{-1} by HF/6-31++G** method and is responsible for the base peak.

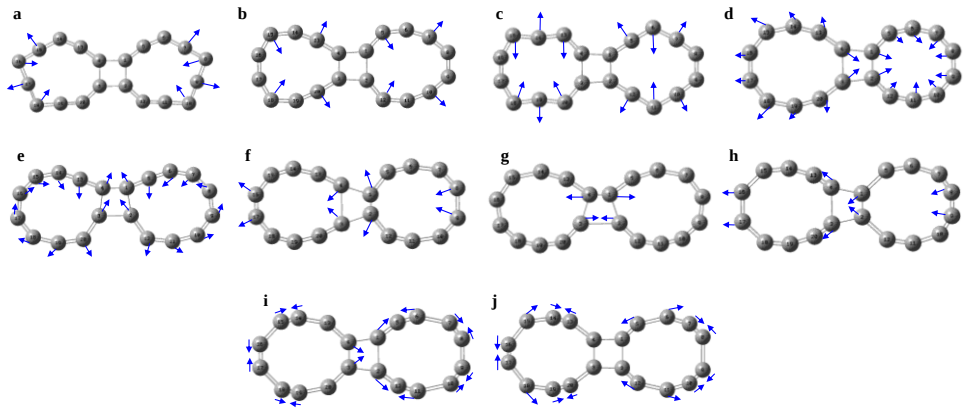

Fig. 5. Vibrational modes for bow-tie isomer at B3LYP/6-31++G level of theory

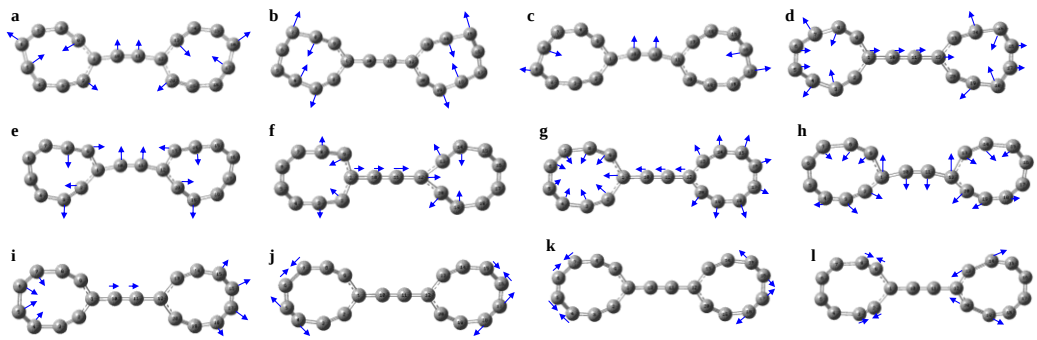

Fig. 6. Vibrational modes for dumb-bell isomer at B3LYP/6-31++G level of theory

The vibrational modes of dumb-bell isomer are shown at Figure 6. The cumulenic double bonds connecting two rings in this isomer (C1=C10=C11=C12) is specific functional group (Figure 2). Bending of this group are responsible for the modes at 171, 430, 491 and 966 cm^{-1} (Figures 6a, c, e, h) and stretching modes are responsible the peaks at 486, 586, 716, and 996 cm^{-1} (Figures 6d, f, g, i) at B3LYP/6-31++G level. The bending vibration of angle ∠C9-C1-C2 and ∠C13-C12-C20 (Figure 2) are responsible for the appearance of characteristic bands of this isomer at 486 and 586 cm^{-1} (Figures 6d, f). The wagging vibration of middle bonds is seen at 966 cm^{-1} (Figure 6h) and assigned as the second characteristic bending vibration of this isomer. The independent stretching vibration of middle carbon atoms is not seen at B3LYP/6-31++G calculation while, this vibrational mode is observed at 1817 and 1928 cm^{-1} by HF/6-31++G and PM3 levels, respectively. In comparison with the previous isomers, the base peak for dumb-bell is assigned to the rings stretching vibrations. The base bands observed at 2061 and 1965 cm^{-1} (Figure 6j) were calculated at B3LYP/6-31++G** and HF/6-31++G**. The base peaks appeared at 2077 and 2282 cm^{-1} (Figure 6k) were calculated at B3LYP/6-31++G and AM1. The base bands observed at 2423 and 2342 cm^{-1} (Figure 6l) were calculated at HF/6-31++G and PM3, respectively.

Spiro isomer has the most number of vibration modes (Figure 7). The observed vibrational modes at 342 and 384 cm^{-1} calculated at B3LYP/6-31++G level (Figure 7a, b) are assigned to the scissoring vibration of the eleven-membered ring carbon atoms. A specific mode corresponding to the bending vibration of the ten-membered ring terminal atoms is seen at 410 cm^{-1} (Figure 7c). The presence of a tetrahedral carbon atom, connecting two rings, results the formation of the specific vibrational modes for this isomer. The bending vibration of angle ∠C11-C1-C20 (Figure 2) can be seen at 544 cm^{-1} (Figure 7i) and its stretching vibrations in the range of 774-1337 cm^{-1}. There is also a specific band corresponding to the bending vibration of tetrahedral carbon atom at 1342 and 1308 cm^{-1} predicted by AM1 and PM3

methods, respectively. The base peak is given by HF/6-31++G** at 481 cm^{-1} (Figure 7e), calculated by B3LYP/6-31++G** at 466 cm^{-1} (Figure 7g), by B3LYP/6-31++G and HF/6-31++G at 527 and 635 cm^{-1} (Figure 7h) and by AM1 and PM3 at 1246 and 1210 cm^{-1} (Figure 7n), respectively. Finally, the stretching vibrations of ring atoms are observed at above 1822 cm^{-1} by B3LYP/6-31++G method.

The IR spectrum of propellane isomer calculated at B3LYP/6-31++G level is very simple. The functional group bands corresponding to the bending vibrations of triangle structure C3-C1(C9)-C15 (Figure 2) are observed at 717 and 783 cm^{-1} (Figures 8a, c) and their stretching vibration as another characteristic of this isomer is seen at 2210 cm^{-1} (Figure 8f). The propellane IR spectrum calculated at HF/6-31++G level is more complex. The scissoring bands are observed in the range of 540-674 cm^{-1} and the other bending vibrations are seen in the range of 1116-1916 cm^{-1}. There are also many stretching vibrations which the peak at 2363 cm^{-1} is the base peak. This peak is given at 1362 cm^{-1} by AM1 calculations which are proportional to the vibration modes of Figures 8d, e. The base peak by PM3 level is a scissoring vibration observed at 543 cm^{-1}.

Vibrational modes for bowl isomer are shown in Figures 9a-k. The base peak at 561 cm^{-1} at B3LYP/6-31++G level (Figure 9a) is assigned to the bending vibration of edge atoms of bowl. This band is observed at 512, 418 and 651 cm^{-1} by B3LYP/6-31++G**, HF/6-31++G** and PM3 calculations, respectively. The bands corresponding to the bending vibration of five-membered ring, as a functional group, are observed in the range of 1390-1469 cm^{-1} (Figures 9g-k). The important point of the IR spectrum of the bowl isomer is the presence of some bands in the range of 500-1600 cm^{-1} by all theoretical levels employed in this work. The base peak predicted by HF/6-31++G and PM3 is seen at 572 and 651 cm^{-1}, respectively (Figures 9a, b). Two new bands at 692 and 700 cm^{-1} are identified corresponding to the simultaneous out of plane bending vibration of five-membered ring and six-membered rings at AM1 calculations. The base peak at 1771 cm^{-1} by AM1 level is assigned to the stretching vibrations of edge atoms of bowl isomer. The stretching mode corresponding to five-membered ring was not detected in any of these calculations. These results reveal that stretching frequencies of carbon in bowl isomer has been shifted to very low frequencies.

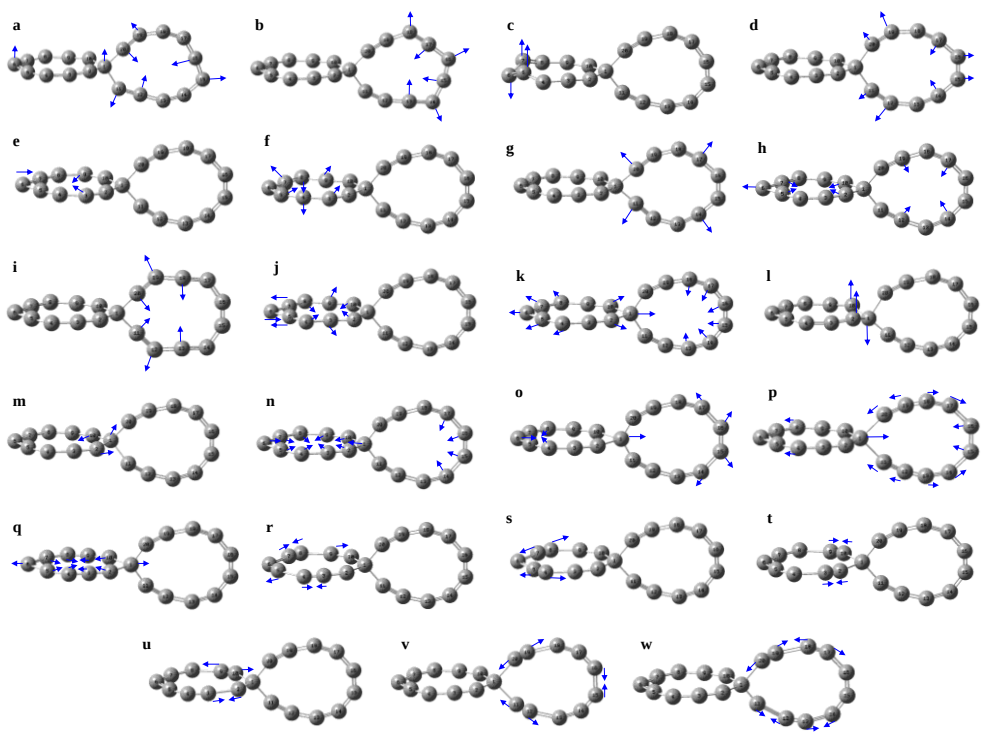

Fig. 7. Vibrational modes for spiro isomer at B3LYP/6-31++G level of theory

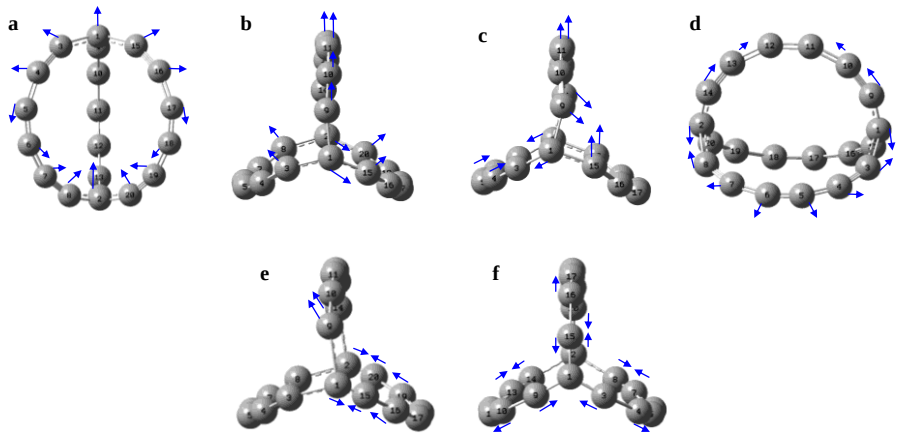

Fig. 8. Vibrational modes for propellane isomer at B3LYP/6-31++G level of theory

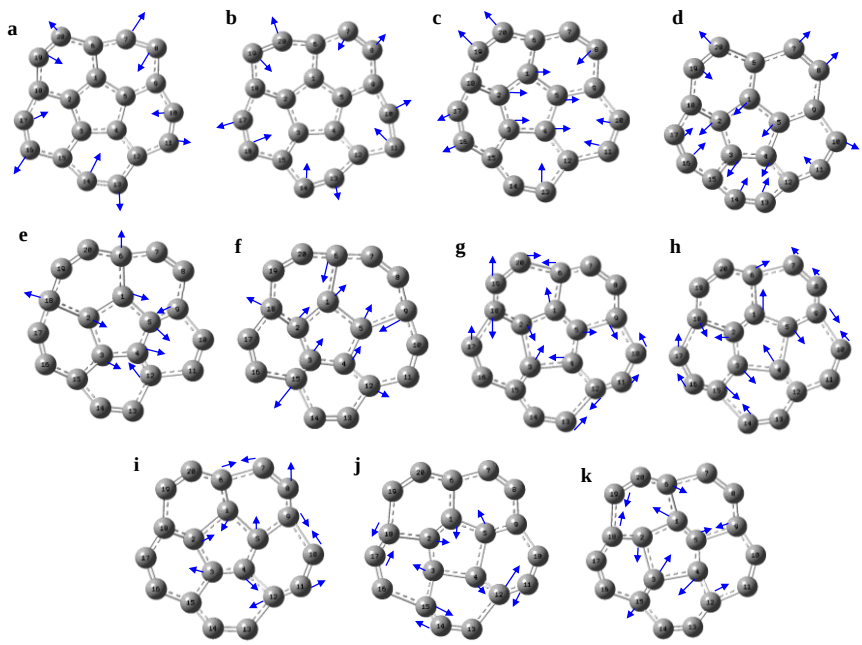

Fig. 9. Vibrational modes for bowl isomer at B3LYP/6-31++G level of theory

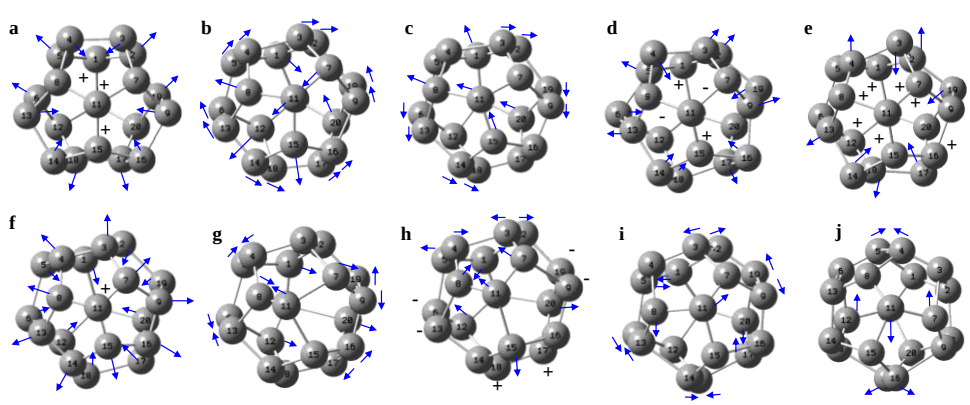

Fig. 10. Vibrational modes for cage isomer at B3LYP/6-31++G level of theory

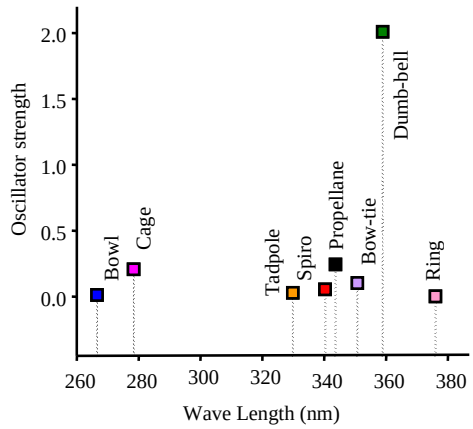

Fig. 11. λ_{max} magnitude for UV spectra of C_{20} isomers

The IR spectrum of the cage isomer calculated at B3LYP/6-31++G level shows wave number in the region 562-1268 cm^{-1} (Figures 10a-h) which all assigned to the bending vibration of carbon atoms. The base peaks at B3LYP/6-31++G and HF/6-31++G levels are observed at 1336 and 1479 cm^{-1} (Figure 10i), respectively and assigned to the stretching vibrations of carbon atoms. The base peaks at B3LYP/6-31++G**, HF/6-31++G**, AM1 and PM3 levels are seen at 1355, 1506, 1490 and 1516 cm^{-1}, respectively. In the cage isomer, the bands corresponding to the stretching modes are very close to bending frequencies such a way that they are merged.

The wavelength and oscillator strength for C_{20} isomers are shown in Figure 11. The ring UV spectrum has two peaks with the same intensity at 376 nm. The number of UV peaks increase for tadpole isomer. The peaks are observed as two sets below and above 376 nm. The maximum of absorption (λ_{max}) for bowl, cage, tadpole, spiro, propellane, bow-tie and dumb-bell is observed at 266.53, 278.37, 329.88, 340.35, 343.71, 350.73 and 358.94, respectively. These results reveal that in UV spectrum belong to monocyclic and bicyclic rings; all transitions are above 300 nm. There is only one transition below 300 nm for tricyclic ring of propellane which is not the main transition while, bowl and cage the absorption maximum transitions are below 300 nm.

4. Conclusions

In summary, we introduce some IR bands as a characteristic of each C_{20} isomer; in other words we verify some specific functional groups, consist of carbon atoms, for C_{20} carbon nanostructures and then, interpret the IR spectra according to them. A broad range of IR spectrum, 400 to 2700 cm^{-1}, is covered by C-C bending vibrations (low frequency region) and C-C stretching vibrations (high frequency region) for all the isomers. The stretching vibrational modes from ring to other isomers (tadpole, bicyclic and tricyclic rings, bowl and cage) are shifted to lower frequencies. The absorption maximum (λ_{max}) in UV spectra for bowl and cage isomers appears below 300 nm and for cyclic isomers above it.

Acknowledgements

We would like to thank the research committee of Malek-ashtar University of Technology (MUT) and Isfahan University of Technology (IUT) for supporting this work. Also, we thank the Computational Nanotechnology Supercomputing Centre, Institute for Research in Fundamental Sciences (IPM), P. O. Box 19395-5531, Tehran, Iran for their kindly supporting in performing some of the computations.

References

1. H. Prinzbach, F. Wahl, A. Weiler, P. Landenberger, J. Worth, L.T. Scott, M. Gelmont, D. Olevano, and B. von Issendorff, Nature, 407, 60-63 (2000).
2. H. Prinzbach, F. Wahl, A. Weiler, P. Landenberger, J. Worth, L.T. Scott, M. Gelmont, D. Olevano, F. Sommer, and B. von Issendorff, Chem. Eur. J., 12, 6268-6280 (2006).
3. Z. Wang, X. Ke, Z. Zhu, F. Zhu, M. Ruan, H. Chen, R. Huang, and L. Zheng, Phys. Lett. A, 280, 351-356 (2001).
4. Z. Slanina, and L. Adamowicz, Fullerene Sci. Tech., 1, 1-9 (1993).
5. G. von Helden, M.T. Hsu, and N.G. Gotts, Chem. Phys. Lett., 204, 15-22 (1993).
6. E.J. Bylaska, P.R. Taylor, R. Kawai, and J.H.J. Weare, Phys. Chem., 100, 6966-6972 (1996).
7. P.R. Taylor, E.J. Bylaska, J.H. Weare, and R. Kawai, Chem. Phys. Lett., 235, 558-563 (1995).
8. K. Raghavachari, D.L. Strout, G.K. Odom, G.E. Scuseria, J.A. Pople, B.G. Johnson, and P.M.W. Gill, Chem. Phys. Lett., 214, 357-361 (1993).
9. J.C. Grossman, L. Mitas, and K. Raghavachari, Phys. Rev. Lett., 75, 3870-3874 (1995).
10. A.H. Romero, D. Sebastiani, R. Ramirez, and M. Kiwi, Chem. Phys. Lett., 366, 134-140 (2002).
11. C. Allison, and K.A. Beran, J. Mol. Struc. Theochem, 680, 59-63 (2004).
12. S. Xu, M. Zhang, Y. Zhao, B. Chen, J. Zhang, and C.J. Sun, Mol. Struc. Theochem, 760, 87-90 (2006).
13. R.O. Jones, J. Chem. Phys., 110, 5189-5200 (1999).
14. Z. Wang, P. Day, and R. Pachter, Chem. Phys. Lett., 248, 121-126 (1996).
15. S. Grimme, and C. Mück-Lichtenfeld, Chem. Phys. Chem., 2, 207-210 (2002).
16. S. Sokolova, A. Lüchow, and J.B. Anderson, Chem. Phys. Lett., 323, 229-233 (2000).
17. G.J. Miller, and J.G.J.Verkade, Math. Chem., 33, 55-79 (2003).
18. L. Turker, J. Mol. Struc. Theochem, 625, 169-171 (2003).
19. Z. Wang, K. Lian, S. Pan, and X. Fan, J. Comput. Chem., 26, 1279-1283 (2005).
20. B. Paulus, Phys. Chem. Chem. Phys., 5, 3364-3367 (2003).
21. E. Maolepsza, H.A. Witek, and S. Irle, J. Phys. Chem. A, 111, 6649-6657 (2007).
22. G. Galli, and F. Gygi, Phys. Rev. B, 57, 1860-1867 (1998).
23. W. Zhi-Gang, Z. Cun-Hua, F. Xian-Hong, P. Shou-Fu, Y. Bing, and J. Ming-Xing, Chinese Phys., 14, 1622-1625 (2005).
24. C. Ze-Xian, Chinese Phys. Lett., 18, 1060-1063 (2001).
25. X.Z. Ke, Z.Y. Zhu, F.S. Zhang, F. Wang, and Z.X. Wang, Chem. Phys. Lett., 313, 40-44 (1999).
26. B.N. Cyvin, E. Brendsdal, J. Brunvoll, and S.J. Cyvin, J. Mol. Struc., 352, 481-488 (1995).
27. J.M.L. Martin, J. El-Yazal, and J. François, Chem. Phys. Lett., 248, 345-352 (1996).
28. F. Varga, L. Nemes, and G.I. Csonka, J. Mol. Struc., 376, 513-523 (1996).
29. M.C. Domene, P.W. Fowler, D. Mitchell, G. Seifert, and F. Zerbetto, J. Phys. Chem. A, 101, 8339-8344 (1997).
30. K.R. Greene, and K. A. Beran, J. Comput. Chem., 23, 938-942 (2002).
31. K.A. Beran, J. Comput. Chem., 24, 1287-1290 (2003).
32. J.I. Chavez, M.M. Carrillo, and K.A. Beran, J. Comput. Chem., 25, 322-327 (2003).
33. M.J. Frisch, G.W. Trucks, H.B. Schlegel, G.E. Scuseria, M.A. Robb, J.R. Cheeseman, J.A. Montgomery, Jr.T. Vreven, K.N. Kudin, J.C. Burant, J.M. Millam, S.S. Iyengar, J. Tomasi, V. Barone, B. Mennucci, M. Cossi, G. Scalmani, N. Rega, G.A. Petersson, H. Nakatsuji, M. Hada, M. Ehara, K. Toyota, R. Fukuda, J. Hasegawa, M. Ishida, T. Nakajima, Y. Honda, O. Kitao, H. Nakai, M. Klene, X. Li, J.E. Knox, H.P. Hratchian, J.B. Cross, C. Adamo, J. Jaramillo, R. Gomperts, R.E. Stratmann, O. Yazyev, A.J. Austin, R. Cammi, C. Pomelli, J.W. Ochterski, P.Y. Ayala, K. Morokuma, G.A. Voth, P. Salvador, J.J. Dannenberg, V.G. Zakrzewski, S. Dapprich, A.D. Daniels, M.C. Strain, O. Farkas, D.K. Malick, A.D. Rabuck, K. Raghavachari, J.B. Foresman, J.V. Ortiz, Q. Cui, A.G. Baboul, S. Clifford, J. Cioslowski, B.B. Stefanov, G. Liu, A. Liashenko, P. Piskorz, I. Komaromi, R.L. Martin, D.J. Fox, T. Keith, M.A. Al-Laham, C.Y. Peng, A. Nanayakkara, M. Challacombe, P.M.W. Gill, B. Johnson, W. Chen, M.W. Wong, C. Gonzalez, and J.A. Pople, Gaussian 03, Revision B.02, Gaussian, Inc., Pittsburgh PA, 2003.